

# INFLUENCE OF THE DYNAMIC BEHAVIOUR OF HELIUM IN THE SHIELDING GAS ON THE WELD BEAD GEOMETRY OF CARBON STEEL GMAW

Rafael Ferezim Morales, [rfmorales@mecanica.ufu.br](mailto:rfmorales@mecanica.ufu.br)

Diandro Bailoni Fernandes, [diandro@mecanica.ufu.br](mailto:diandro@mecanica.ufu.br)

Américo Scotti, [ascotti@mecanica.ufu.br](mailto:ascotti@mecanica.ufu.br)

Federal University of Uberlândia, School of Mechanical Engineering, Laboratory for Welding Process Development (LAPROSOLDA), João Naves de Ávila Av., 2160 - Campus Santa Mônica, ZIP: 38400-902, Uberlândia, MG, Brazil,,

**Abstract.** Several shielding gas blends are used in industrial applications of the GMAW process. The bead geometry is one of the criteria for shielding gas selection, always taking into account the economical factor. The objective of this work was the assessment of the influence of He addition (more expensive) in the composition of the shielding gas over the weld bead geometry in carbon steel GMAW. This study was carried out using an Ar+5%O<sub>2</sub> blend, with and without 25% He addition. Bead-on-plate welds were carried out for each gas combination at two distinct arc lengths and at one current level (spray transfer). Metal transfer characteristics (droplet arrival speed, size and detachment rate) were quantified by using high-speed filming and especial softwares. Quantity of Movement of the droplets transferred by unit of weld length were calculated and correlated to bead geometric profiles (penetration, bead width, reinforcement and fusion area), which were determined from test plate cross sections. The results showed that He in the shielding gas composition does not affect either the bead geometry or the Quantity of Movement, independently of the arc length. This does not confirm the thermal and mechanical effect that He could have on carbon steel GMAW.

**Keywords:** GMAW; shielding Gas, Bead Geometry, Helium, Argon, Quantity of Movement.

## 1. INTRODUCTION

In industrial applications of the GMAW process, several types of shielding gases are used, from single component ones to mixtures of up to four components of gases (Suban & Tusek, 2001). The preliminary function of the gaseous protection is to exclude the atmosphere of the contact with the metal melted. That is necessary because most of metals, when heated up to its fusion point in presence of air, exhibits a strong tendency to form oxides and nitrites (gaseous and/or solid) (AWS, 1991). Argon (Ar) and Helium (He) are examples of shielding gases used alone or as components of mixtures in the GMAW process. Both are inert, but they present quite different properties, as ionization potential (which reflects the easiness of the gas for ionizing), density and thermal conductivity. Thus, they should proportionate uneven characteristics during arc welding.

According to Lancaster (1984), the first ionization (that represents the loss of an electron) potentials for Ar and He are 15.755 and 24.580 eV, respectively. A smaller potential of ionization of the Ar indicates that it is ionized by demanding less energy when compared to He and, consequently, the arc can be struck and maintained easier. On the other hand, the highest potential of ionization of He requests higher voltage to ionize the gas and to supply the current flow to sustain the arc (Jönsson, 1995) and, in consequence, higher electrical power (and welding energy) is obtained. It is generally accepted that gases with higher ionization potential leads to higher penetration, due to the ionization enthalpy which would be higher and the energy delivered to the plate when the plasma contact it.

The density of the gas plays an important role in the protection of the arc and fused puddle against the atmosphere (Suban & Tusek, 2001), since it interferes in the speed and in the flow profile of the gases. Ar is approximately 1.4 times denser than the atmospheric air, while the density of He is approximately 0.14 times (AWS, 1991). In other words, when He is used as a shielding gas, the flow is requested to be two to three times higher to make an equivalent protection as Ar (AWS, 2000). Due to that property of the Ar (pure or in mixtures) is considered to promote better protection. The thermal conductivity is another significant characteristic. Fig 1 displays the thermal conductivity of the more frequently used gases in function of the temperature, in which one can notice that He has a larger thermal conductivity than the Ar in high temperatures. It is believed that in function of this property, He produces a plasma arc in which the energy is more evenly distributed. The arc of Ar plasma, on the other hand, is characterized by an internal section of high energy and an external volume of low energy.

Based on these characteristics of He in relation to Ar (higher thermal conductivity and ionization potential), one should expect different performance when one gas is used to replace the other. According to the AWS handbook (1991), typical bead profiles for Ar and He GMAW welds are as illustrated by Fig. 2. Pure He does not show to improve penetration, besides making the metal transfer unstable. In the other side, pure Ar leads to "finger like" beads. Helium has been indicated for welding applications in which it is necessary a higher thermal contribution to improve the wettability of the fused bead (less convex profiles) and to reach larger penetrations or higher welding speeds. Norrish (1992), for instance, mentioned the use of He in the industry for materials of high conductivity, due to capacity of producing high-speed welds. Scotti (1998) cites that the reason for this performance is the fact that He produces a

more concentrated arc and smaller cathode spot, resulting in greater penetration. Still cites that Ar demands lower voltage for the same arc length and current, presenting a shallower weld penetration and undercutting. However, the cost of the gas He is higher than of Ar, what is a commercial disadvantage. Besides, Ar tends to produce more stable arcs than pure He. Thus, due to that instability, the use of pure He is limited to especial applications (AWS, 2000).

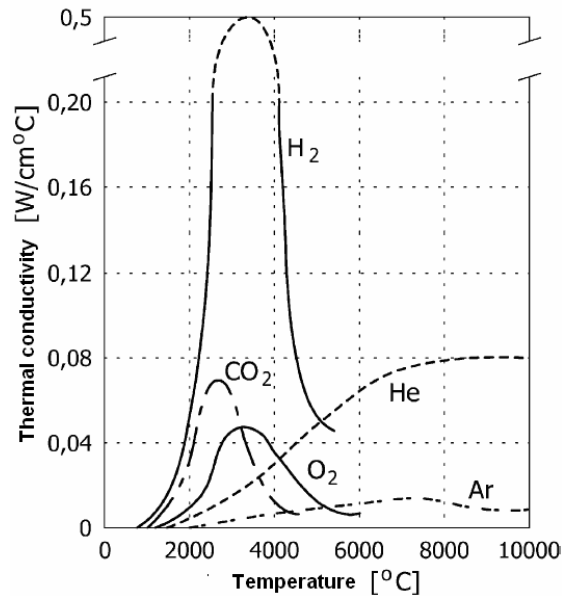


Figure 1 - Thermal Conductivity of gases at 1 atm (Lancaster, 1984).

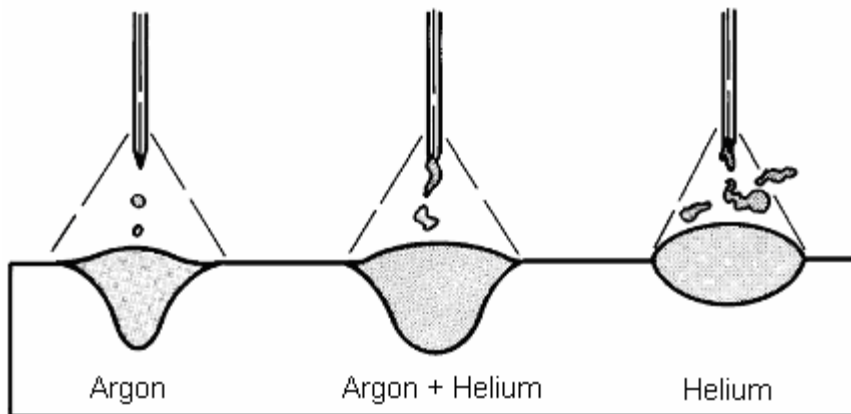


Figure 2 - Typical bead profiles for Argon and Helium (AWS, 1991).

In a previous work (Morales et al, 2007), it was demonstrated that He in mixture with Ar+5%O<sub>2</sub> did not affect the geometry of beads (bead-on-plate) on carbon steel. However, there were no explanation for the fact that so different gases could have similar behavior in relation to the thermal contribution to the bead formation in steel GMAW, yet the arc seemed to be unlike (the blend with He showed more spattering). One characteristic could have balanced the expected performance of He concerning its higher delivered thermal properties, namely the influence on the quantity of movement of the impinging droplets. Thus, the objective of the work was an attempt to justify the reason for He in mixture with Ar do not show any increase in the fusion efficiency of the arc during carbon steel GMAW welds.

In brief, the droplets in transfer impinge the fused pool. Droplets have velocity and acceleration when they detach and are further accelerated in their passage across the arc (Lancaster, 1986, p. 206). The initial velocity of a drop as it leaves the wire can be accounted for the wire velocity and both the stored surface tension energy and the imparted momentum created by static forces at the electrode tip (Clark et al., 1989, Johnson et al, 1991). When they collides the pool, their quantity of movement, also known as Momentum (mass x speed), is transferred to the bead on formation. Droplets not only have quantity of movement but also carry approximately 47% of the total heat which is transferred by the process to the weld pool (Clark et al., 1989, Watkins, 1992). As a result, droplets promote fluid motion in the weld pool. Therefore, droplet size and detachment frequencies are key factors in the welding process performance. Kin & Na (1995) verified that when melted electrode droplets were included in their bead shape modeling, the depth of predicted penetrations was considerably increased and the results matched closer the practical ones.

The quantity of movement of a droplet ( $M_{drop}$ ) can be defined as Eq. (1):

$$M_{drop} = \rho \cdot \frac{\pi \cdot d^3}{6} \cdot V_{arriv} \left[ \frac{kg \cdot m}{s} \right] \quad (1)$$

where " $\rho$ " is the density of the droplets (7850 kg/m<sup>3</sup>), "d" the mean diameter of the droplet and " $V_{arriv}$ " the mean speed of the droplets arriving the pool. The larger the quantity of movement, more mechanical energy would be transferred to the pool by the droplets. However, as the droplets are formed in sequence at a given frequency ("f"), the energy transfer happens continuously along the time. Thus, one can define by Eq. (2) the force "F" that acts on the pool due to the impact of the droplets. If this force "F" is divided by the welding travel speed (TS), it is possible to reach what the authors denominate "Quantity of Movement Transferred by Unit of Weld Length" or "Effective Quantity of Movement", referred here by  $M_{effec}$ , given by Eq. (3).

$$F = M_{drop} \cdot f \left[ \frac{kg \cdot m}{s^2} \right] \quad (2)$$

$$M_{effec} = \frac{F}{TS} \left[ kg \cdot m \cdot s^{-1} \cdot m^{-1} \right] \quad (3)$$

## 2. EXPERIMENTAL PROCEDURES

To study the influence of the dynamic behavior of He addition in the shielding gas on the profile of the weld bead, a mixture of Ar+5%O<sub>2</sub> was taken as reference. This gas blend is typically suitable for GMAW of carbon steel working in spray transfer. The comparative blend was an Ar+5%O<sub>2</sub>+25%He. These gas mixtures were prepared using a laboratory gas mixer, set for a flow of 14 l/min. A same current level (I) and wire feed speed (WFS) was employed in both cases. For that, a multiprocess electronic power source (secondary chopper) was programmed to work at the constant current mode to guarantee the same current value in all comparative experiments. In this way, the values of I and WFS were set, while voltage was the resultant from the loading (characterized by each arc). This operational approach also allows obtaining different arc lengths through variations of the Contact Tip to Work Distance (CTWD); for a given I and WFS, the longer the CTWD, the longer the arc length. Two different arc lengths were searched for each welding condition (gas composition, at same I and WFS).

Bead-on-plate welds were carried out on 200 x 25.4 x 9.5 mm plain carbon steel plates (ABNT 1020), using an AWS ER70S-6 wire of 1.2 mm. The Table 1 display the parameters set for each run. Each test plate was split at three different places, resulting in a total of three transverse sections for bead geometric analysis. The cross sections were properly prepared by metallographic etching (Nital 10%) and, using a CCD camera and a image treatment program, the mean values of the main geometric characteristics of the weld beads were taken (reinforcement, penetration, width and fusion area).

Table 1. Parameters for the tests

Runs	Shielding Gas	Setting WFS (m/min)	Travel Speed (cm/min)	CTWD (mm)	Setting Current (A)
01	Ar + 5%O <sub>2</sub>	6.9	40.8	24	250
02	Ar + 5%O <sub>2</sub> + 25%He	6.9	40.8	24	250
03	Ar + 5%O <sub>2</sub>	6.9	40.8	18	250
04	Ar + 5%O <sub>2</sub> + 25%He	6.9	40.8	18	250

In order to pursuit the objectives of the work, it was necessary to measure the arc lengths (to guaranty that the two levels were obtained and they would be approximately the same for the two gas compositions), the droplet sizes and frequencies and the speeds of droplet approaching the weld pool (those three parameters to calculates the quantity of movement, as it will be seen later). The measurements were possible by using the Shadowgraphy technique illustrated in Fig. 3 (presented by Lin et all, 2000, and several other authors). Figure 4 gives more details of the rig, in which a He-Ne laser (632,2 nm) beam are used to project the shadow of several elements (torch, electrode, droplets and weld pool) directly on the lens of a high-speed (2000 pictures a second) digital camera.

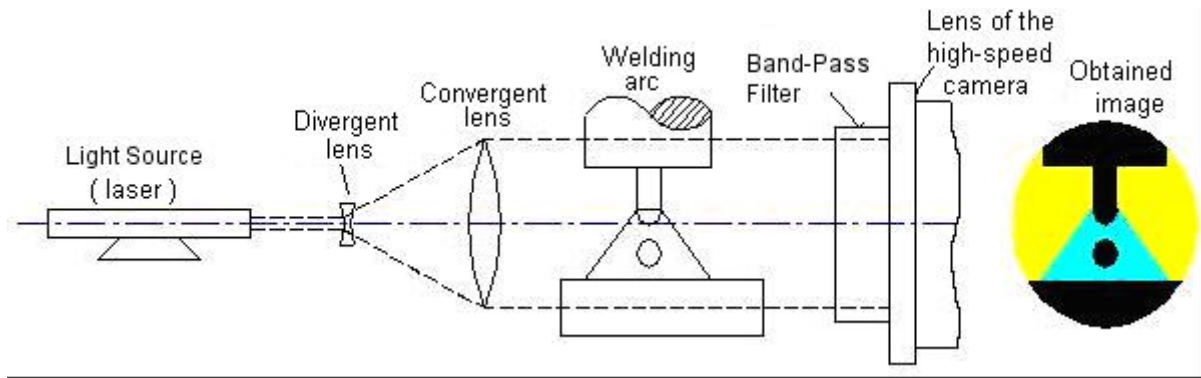


Figure 3 - The principle of the Shadowgraphy technique applied to welding , also known as "Back-lighting" (Bálsamo et al, 2000).

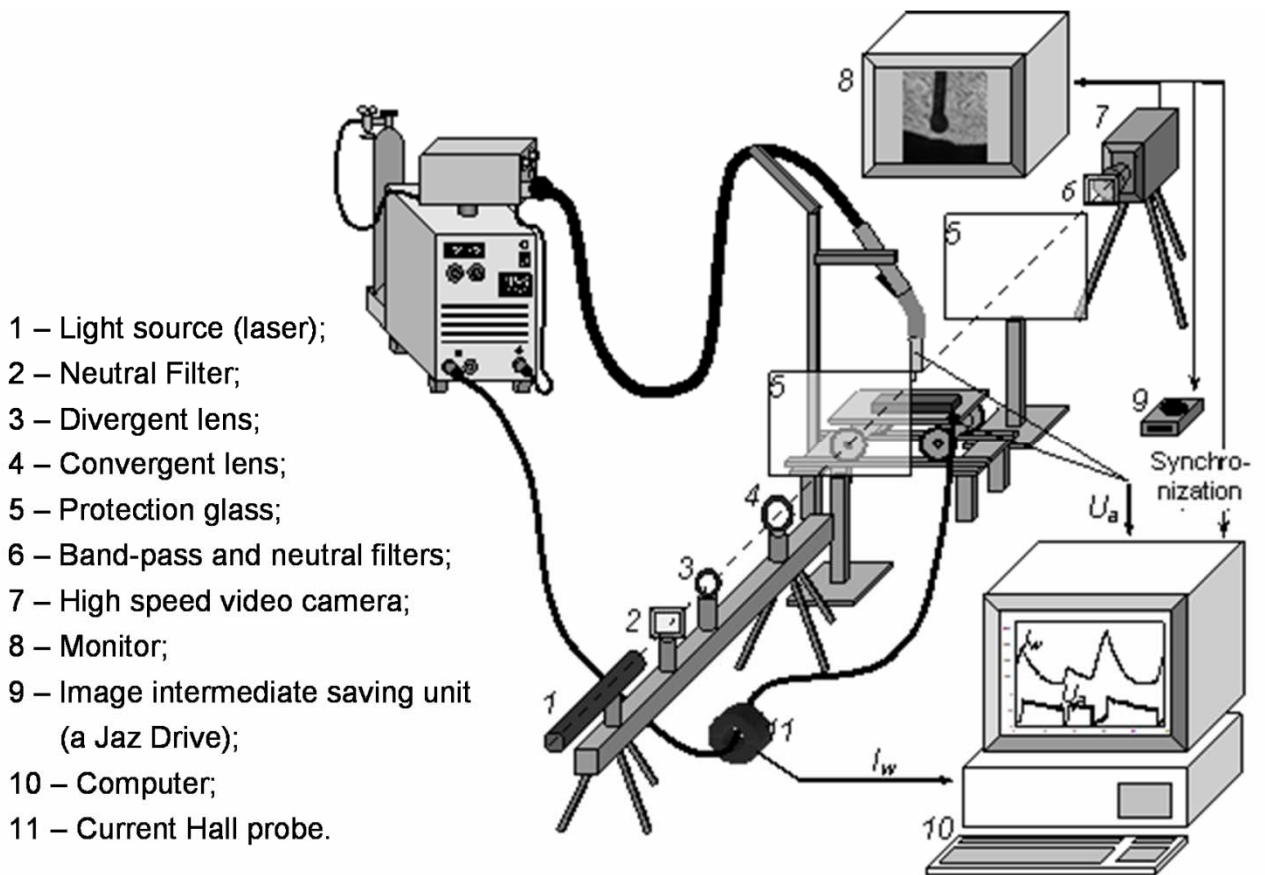


Figure 4 - Details of the laser-optical system used in the experiments.

The images of the high-speed filming are treated by a home made dedicated software (Maia et al, 2000 e 2003). This computer tool, as illustrated in Fig. 5, is an interactive software that analyzes quantitatively the geometric and dynamic characteristics of the objects in the images of metallic transfer in GMAW, such as droplet detachment rate and size, arc and electrode stick-out lengths, etc. In this work, 10000 frames the metal transfer image were analyzed by the program to define the average values of the above mentioned quantities (equivalent to 5 seconds of each event). The kinetic characteristics of the metallic transfers (mainly droplet speeds) were measured through another software, OPTIMAS MA 1.4 (commercial), which use a sequence of images TIFF, as shown in Fig. 6, to make calculations and to supply the space position and the speed and instantaneous acceleration of each droplets along the time. The data supplied by both programs (vectorial) are saved in tables that can be treated in electronic spreadsheets. The goal of this kinetic measurement was the average speed value of the droplet arriving into the weld pool. For that, 9 frame sequences of one droplet traveling from the electrode end to the pool were randomly (yet fixing a constant interval among each analysis) taken for each run. This number for sampling was confirmed as correct according to the criterion of determination of the minimum number of samples for small populations, with a level of trust of 95%, according to the distribution "t" of Student. The average value represents mean of the mean speed of the droplets at 2 frames before reaching the pool.

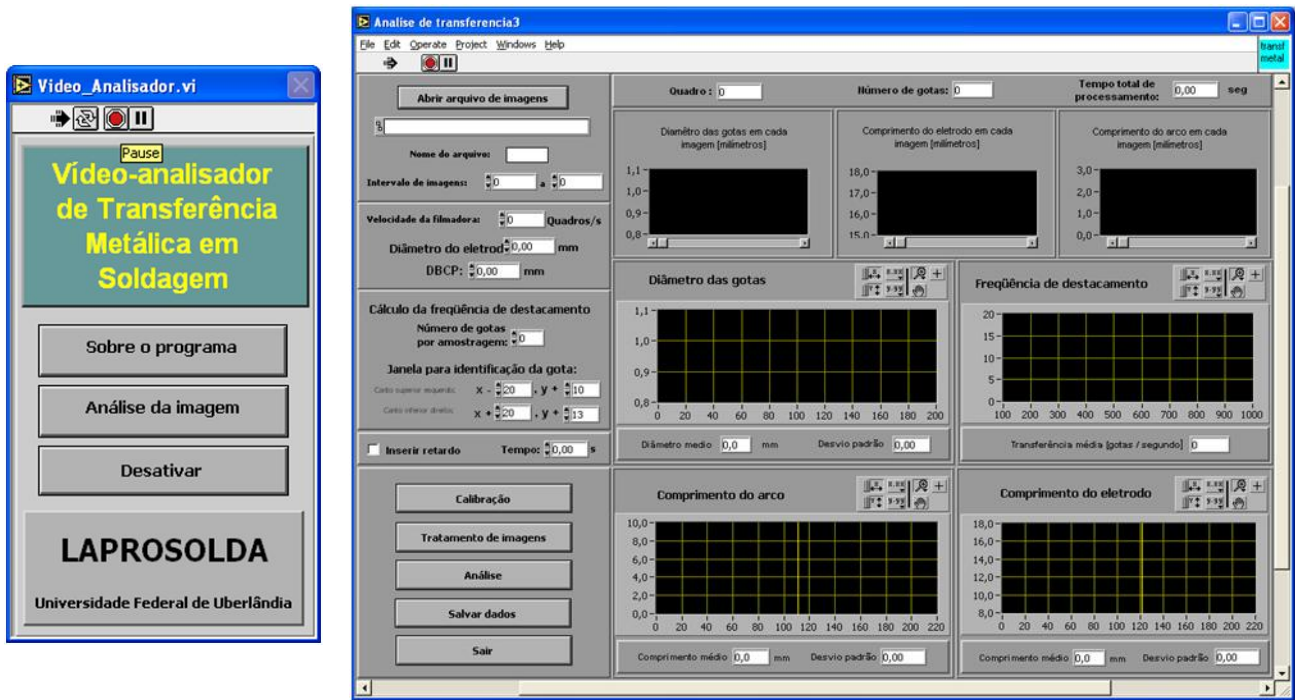


Figure 5 – Screens of the Metal Transfer Analyzer software.

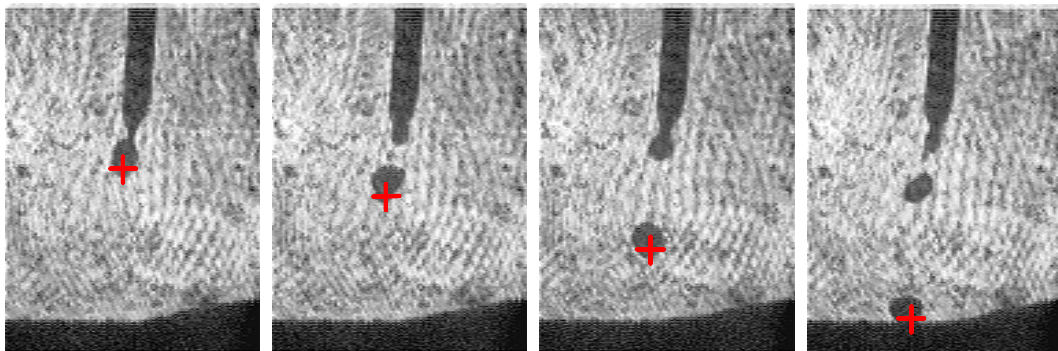


Figure 6 - Sequence of metallic transfer, with the definition of the target.

### 3. RESULTS AND DISCUSSION

Figure 7 illustrates the behavior of the droplets traveling along the arc length for the four runs. The Table 2 presents the mean values of voltage, current, arc length, droplet diameter, frequency and arrival speed, regarding each one of the four accomplished runs. It is important to point out that the figures presented in Tab. 2 carries some measurement intrinsic errors and not precise geometric assumptions, such as considering the traveling droplet as a sphere. However, calibrations of the filming system and calculation of theoretical droplet sizes are with a reasonable good agreement. The purpose of having approximately same current (around 250 A) and two different levels of arc length (around 7.4 and 11.2 mm) was reached. Fortunately, the gas mixtures did not influenced the arc length for a given CTWD, avoiding the need of finding the same arc lengths by trial and error approach. This means that He at this content does not interfere in an outstanding way on the fusion rate of the electrode-wire, fact no necessarily expected. It can be observed that voltage increases for longer arcs, as much as with the use of He in the blend. These data, as expected, are indications that the experiments were well succeeded. It can also be observed both gas blend and arc length did not have influence on the droplet diameter and even on the arrival speed, considering the data dispersion, but arc length showed to influence the detachment rate.

Table 2 – Average of the measured values resultants from the experiments

Run	Shielding Gas	CTWD (mm)	$I_{rms}$ (A)	$U_{rms}$ (V)	Arc Length (mm)	Droplet Diameter (mm)	Detachment frequency (droplets/s)	Droplet arrival speed (cm/s)
01	Ar + 5%O <sub>2</sub>	24	248	33.6	11.5 ± 0.6	1.2 ± 0.2	281	179 ± 21
02	Ar + 5%O <sub>2</sub> + 25%He	24	244	34.2	11.0 ± 0.6	1.4 ± 0.2	227	144 ± 16
03	Ar + 5%O <sub>2</sub>	18	254	30.2	7.3 ± 0.6	1.2 ± 0.2	328	149 ± 7
04	Ar + 5%O <sub>2</sub> + 25%He	18	252	31.4	7.5 ± 0.5	1.2 ± 0.2	345	145 ± 26

CTWD = contact-tip to work distance;  $I_{rms}$  =monitored rms value of current;  $U_{rms}$  =monitored rms value of voltage.

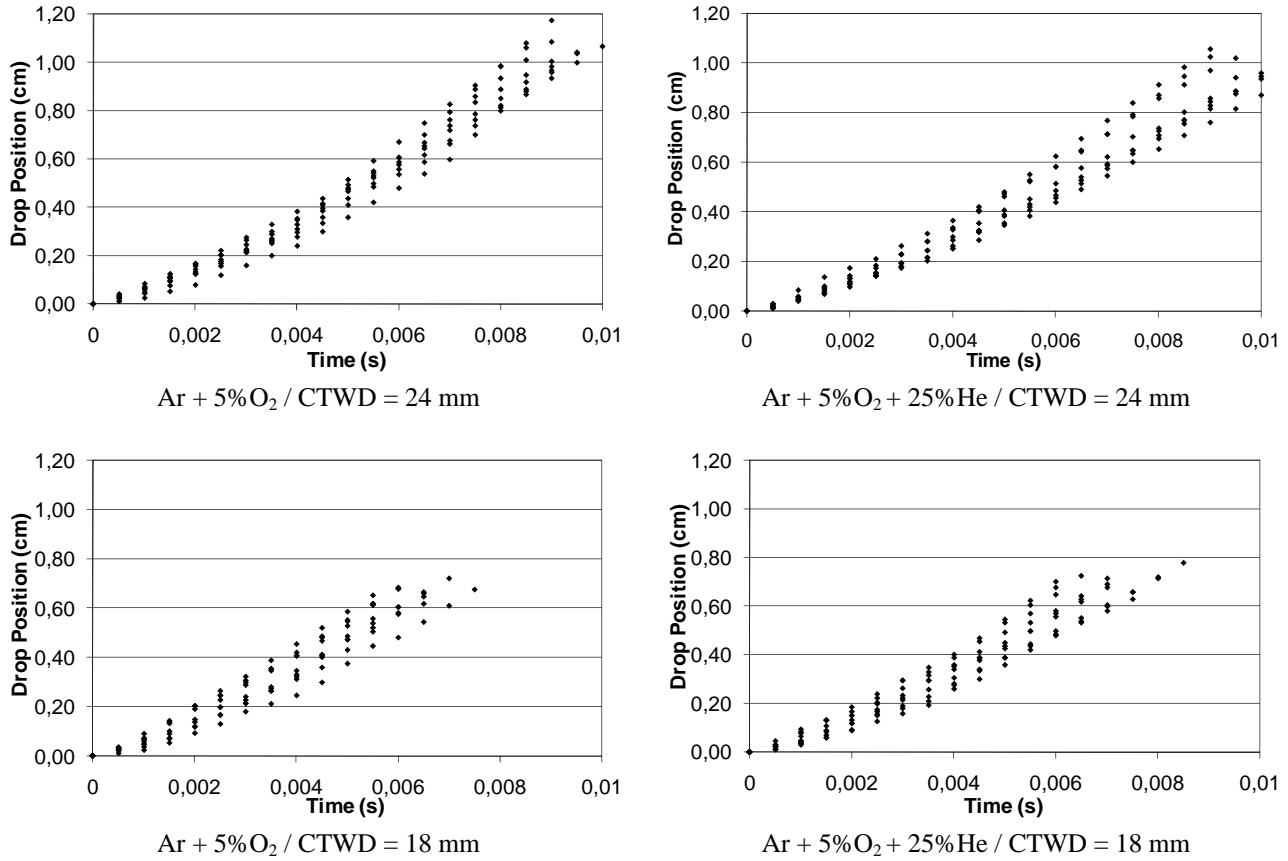


Figure 7 – droplet position as a function of time for the 4 runs, used for calculating the droplet arrival speed

Table 3 presents the analysis of the quantity of movement of single droplets of each run, using data from Tab. 2 applied over Eq. (1) to (3). One could say that the quantity of movement is higher for longer arc, but there is no clear evidence of a He influence. In fact, when Effective Quantity of Movement is on comparison, one can say that there are no significant value variations either due to gas composition or arc length.

Table 3 - Calculated values of quantity of movement of a drop, its collision force on the pool and its effective quantity of movement.

Test	Shielding Gas	CTWD (mm)	Mass of the drop (kg)	Quantity of movement of a drop (kg.m/s)	Force that acts on the pool (N)	Effective Quantity of Movement (kg.m/s/m)
01	Ar + 5%O <sub>2</sub>	24	7,10251E-06	1,27009E-05	0,003568955	0,524846367
02	Ar + 5%O <sub>2</sub> + 25%He	24	1,12785E-05	1,62889E-05	0,003697584	0,543762288
03	Ar + 5%O <sub>2</sub>	18	7,10251E-06	1,05732E-05	0,003468015	0,510002215
04	Ar + 5%O <sub>2</sub> + 25%He	18	7,10251E-06	1,02956E-05	0,003551982	0,522350222

Table 4 illustrates the bead formation resulting from the 4 runs. One can observe that 25% of He was not enough to prevent the “finger-like” bead penetration (in contrast to Fig. 2). It can also be noticed that the aspect of the bead was not affected by the addition of He to the shielding gas, except for some few porosities when He was used together with long arc. However, some differences in bead geometry can be seen between short and long arcs. The quantification of these findings can be observed by Tab. 5 and Fig. 8 to 11. Despite the large standard deviations, but considering similar results in a previous work (Morales et al, 2007), two tendencies can be drawn from these data: a) Shorter arcs and addition of He proportionate wider beads with shorter reinforcements (Fig. 8 and 9), that is, less convex beads; and b) Shorter arcs, independently He content lead to deeper penetration and bigger fusion area (Fig. 10 and 11).

Table 4 - Aspect of the surface and of the traverse section of the weld beads


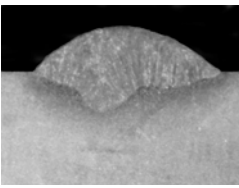

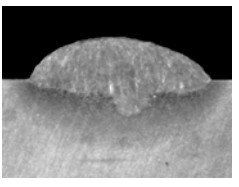

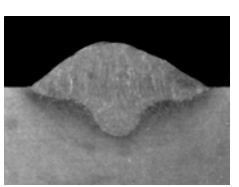

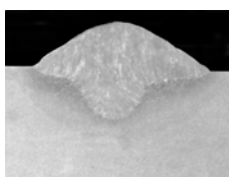
Runs	Shielding gas	Aspect of the weld Bead	Cross section
01	Ar + 5%O <sub>2</sub> (long arc)		
02	Ar + 5%O <sub>2</sub> + 25%He (long arc)		
03	Ar + 5%O <sub>2</sub> (short arc)		
04	Ar + 5%O <sub>2</sub> + 25%He (short arc)		

Table 5 – Mean values of the geometric characteristics of the weld beads (average of 3 cross sections).

Test	Shielding gas	CTWD (mm)	Reinforcement (mm)	Width (mm)	Penetration (mm)	Fusion area (mm <sup>2</sup> )
01	Ar + 5%O <sub>2</sub>	24	2,5	10,6	2,6	12,2
02	Ar + 5%O <sub>2</sub> + 25%He	24	2,3	11,4	2,2	12,0
03	Ar + 5%O <sub>2</sub>	18	2,3	11,3	2,6	13,6
04	Ar + 5%O <sub>2</sub> + 25%He	18	2,1	12,7	2,5	15,6

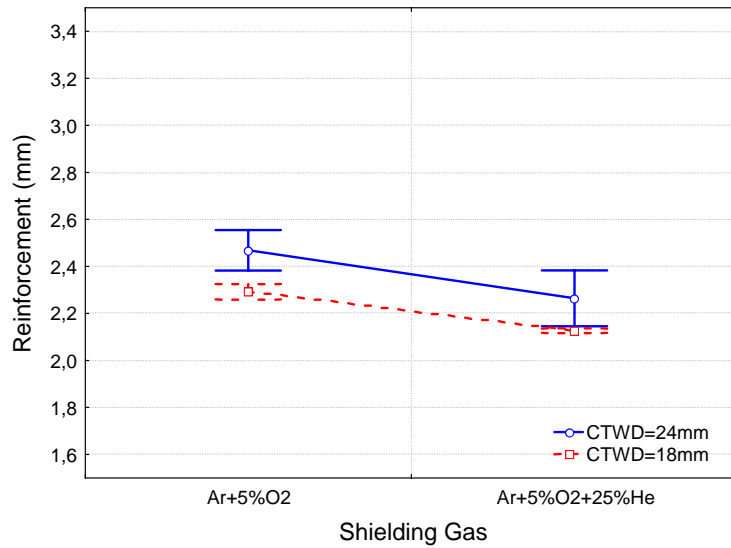


Figure 8 - Reinforcement as a function of the shielding gas compositions.

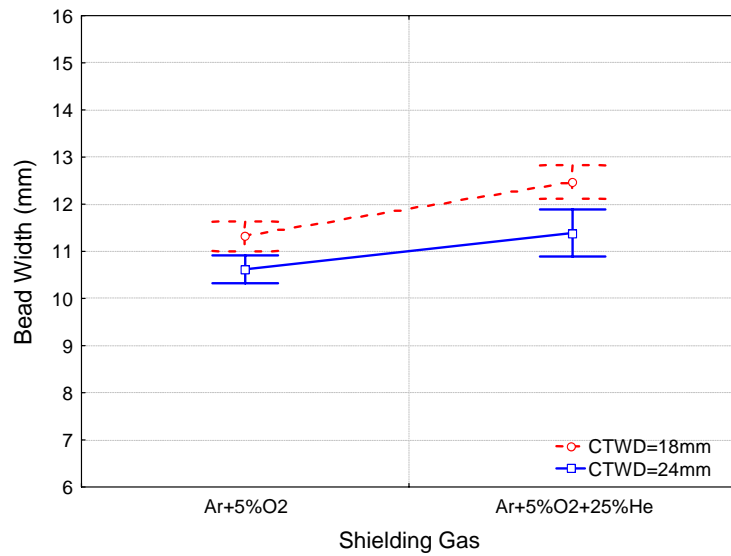


Figure 9 – Bead Width as a function of the shielding gas compositions.

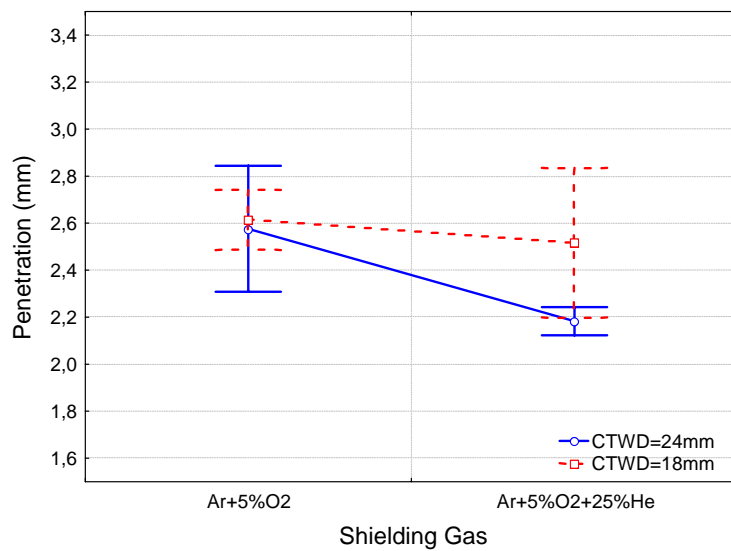


Figure 10 - Penetration as a function of the shielding gas compositions



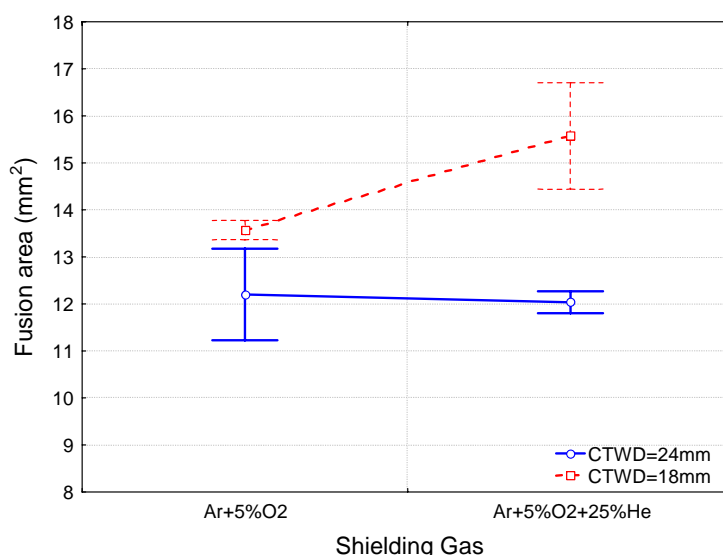


Figure 11 – Fusion area as a function of the shielding gas compositions

As welding current, wire feed rate and travel speed were approximately the same in all experiments, the above mentioned results put in evidence only some importance of the arc length on bead formation, but it is not possible to detect any influence of He addition. In the current literature it is said that the longer the arc the wider and shallower the bead. These tendencies have been related to arc concentration, since a short arc tends to have a smaller base (heat concentration at the cathodic region), resulting in deeper penetration but with less heating alongside the bead (poor wettability and narrower bead). This concept must be treated carefully here (which the results were opposite), since both arc lengths are long enough if compared to those in practical applications. An arc as long as 11 mm might be too long so that the arc coupling to the base metal may not increase much more than for 7-mm-long arcs.

Beside of being small the He addition influence on geometric parameters, it does not seem to be related to mechanical properties (the effective quantity of movement was much the same for all conditions, as seen in Table 3); He addition was not able to chance the kinetic behavior of the droplets. On the other hand, the similar Effective Quantity of Movement may have been the responsible for the “finger-like” profiles of the bead penetrations in all cases.

#### 4. CONCLUSION

In the conditions of this work (current of welding of 250 A – spray transfer - and two levels of long arc lengths, approximately 11 and 7,5 mm) it can be inferred that, at least for mixture of Ar+5%O<sub>2</sub>, the addition of He has no influence on the geometric dimensions of the weld bead. There is only a small influence of the arc length. However, both arc length and He addition did not change the Quantity of Movement of the droplets transferred by unit of weld length (Effective Quantity of Movement). This does not confirm the thermal and mechanical effect that He could have on carbon steel GMAW

#### 5. ACKNOWLEDGMENTS

The authors would like to thank the governmental agencies for research developments: CNPq, for the financial support as scholarship; and FAPEMIG, for the financial support for infrastructure through the Project TEC 604/2005.

#### 6. REFERENCES

- AWS, Supplement: The American Welder, Vol. 79, no. 1-2, , pp. 18. Jan.-Feb. 2000
- AWS (1991), **Welding Handbook: Welding Process (Vol II)**, AWS, USA, 8<sup>th</sup> Edition, cap. 4, 955 p. (ISBN 0-87171-354-3).
- BÁLSAMO, P.S.S., VILARINHO, L. O., VILELA, M. & SCOTTI, A.; **Development of an Experimental Technique for Studying Metal Transfer in Welding: Synchronized Shadowgraphy**, In: Int. J. for the Joining of Materials, vol 12, no. 1, 2000, The European Institute for Joining of Materials (JOM), Denmark, pp. 1-12 (ISSN 0905-6866)
- CLARK, D.E.; BUHRMASTER, C.L. & SMARTT, H.B, **Drop Transfer Mechanisms in GMAW**, 2nd Int. Conf. on Recent Trends in Welding Science and Technology, ASM, Gatlinburg, Tennessee, USA, 14-18 May 1989, pp. 371-375.
- JOHNSON, J.A.; CARSON, N.M, SMART, H.B. & CLARK, D.E., **Process Control of GMAW: Sensing of Metal Transfer Mode**, Welding Journal, Apr 1991, AWS, pp. 91s-99s.
- JÖNSSON, P.G.; T.W. EAGAR, and J. SZEKELY, **Heat and Metal Transfer in Gás Metal Arc Welding Using Argon and Helium**. Metallurgical and Materials Transactions, Volume 26B, April 1995, pp. 383-395.

- KIM, J.W. & NA, S.-J., **A Study on the Effect of Contact Tube-to-Workpiece Distance on Weld Pool Shape in Gas Metal Arc Welding**, Welding Journal, May 1995, AWS, pp. 141s-152s.
- LANCASTER, J.F., **The Physics of Welding**, Chapter 7, 1st Ed., Pergamon Press, Oxford, United Kingdom 1986, ISBN 0-08-030554-7.
- MAIA, T. C. G., FLÔRES, E. L. & SCOTTI, A., **Quantificação da Transferência Metálica no Processo MIG/MAG por Processamento de Imagens**, II Cong. Nacional da Engenharia Mecânica - CONEM 2002, 12 a 16 de Agosto, João Pessoa, UFPa/ABCM, CPB1200, 10 p.
- MAIA, T. C. G., FLÔRES, E. L. & SCOTTI, A., Avaliação Comparativa entre Análises Quantitativas Automatizada e Manual Aplicadas sobre Imagens de Transferência Metálica em Soldagem MIG\MAG, II Congresso Brasileiro de Engenharia de Fabricação – COBEF 2003, ABCM/UFU, Maio de 2003, Uberlândia, MG, CD ROM – artigo COF03\_0520
- MORALES, R. F, RESENDE, A. A., SCOTTI, A. (2007), **Influência da Adição de Hélio no Gás de Proteção sobre a Geometria do Cordão de Solda MIG/MAG de Aço ao Carbono**, IV Congresso Brasileiro de Engenharia de Fabricação, Águas de São Pedro – São Paulo, 2007, CDROM, paper.
- NORRISH, J. (1992), **Advanced Welding Processes**, Institute of Physics Publishing, Bristol, United Kingdom, p. 83.
- Q LIN, X LI & S W SIMPSON, **Metal transfer measurements in gas metal arc welding**. Journal of Physics D: Applied Physics. 2000. pp 347-353.
- SCOTTI, A., **A Review on Special Metal Transfer Modes in GMAW**, Rev. Bras. de Ciências Mecânicas - RBCM, ABCM, vol XX, no. 3, Set 1998, pp. 465-478. (ISSN 0100-7386)
- SUBAN, M.; TUSEK, J. (2001). Dependence of Melting Rate in MIG/MAG Welding on the Type of Shielding Gas Used, **Journal of Materials Processing Technology**, pp 185 - 192.
- WATKINS, A.D.; SMARTT, H.B. & JOHNSON, J.A. (1992), **A Dynamic Model of Droplet Growth and Detachment in GMAW**, 3rd Int. Conf. on Trends in Welding Research, ASM, Gatlinburg, Tennessee, USA, 1-5 Jun 1992, pp. 993-997.